Chapter

CO_2 Reduction Characteristics of Cu/TiO_2 with Various Reductants

Akira Nishimura

Abstract

Cu-doped TiO_2 (Cu/TiO_2) film photocatalyst was prepared by combination of sol-gel and dip-coating process and pulse arc plasma method. The effect of Cu/TiO_2 photocatalyst on CO_2 reduction performance with reductants of H_2O and H_2 or NH_3 was investigated. In addition, the overlapping two Cu/TiO_2 coated on netlike glass discs were also investigated. The CO_2 reduction performance of Cu/TiO_2 film was tested under illumination of Xe lamp with or without ultraviolet (UV) light, respectively. As to the condition of $CO_2/H_2/H_2O$, the best CO_2 reduction performance has been achieved under the condition of $CO_2/H_2/H_2O$ = 1:0.5:0.5 with UV light illumination as well as without UV light illumination. The theoretical molar ratio of CO_2/H_2O or CO_2/H_2 to produce CO is 1:1. Since the molar ratio of $CO_2/H_2/H_2O$ = 1:0.5:0.5 can be regarded as the molar ratio of CO_2/total reductants = 1:1, it is believed that the results of this study follow the reaction scheme of CO_2/H_2O and CO_2/H_2. On the other hand, as to the condition of $CO_2/NH_3/H_2O$, the best CO_2 reduction performance has been achieved under the condition of $CO_2/H_2/H_2O$ = 1:1:1 with UV light illumination as well as without UV light illumination.

Keywords: CO_2 reduction, Cu/TiO_2 photocatalyst, reductants combination, visible light, overlapping effect

1. Introduction

Paris Agreement adopted in 2015 sets the goal that the increase in average temperature in the world from the industrial revolution by 2030 should be kept less than 2 K. However, due to the increase in the averaged concentrations of CO_2 in the atmosphere to 410 ppmV in December 2019 [1], CO_2 reduction or utilization technologies to recycle CO_2 are urgently required.

There are six vital CO_2 conversions: chemical conversions, electrochemical reductions, biological conversions, reforming, inorganic conversions, and photochemical reductions [2, 3]. Recently, artificial photosynthesis or the photochemical reduction of CO_2 to fuel has become an attractive route due to its economically and environmentally friendly behavior [2].

The application of CO_2 as a raw material can produce chemicals and energy to diminish the CO_2 accumulation in the atmosphere [2]. If we consider energy producing possibilities, one possibility is the photochemical conversion of CO_2 into value-added chemicals which could be used as fuel [4].

The most widely used photocatalyst for the photocatalytic reactions is TiO_2 due to its availability, chemical stability, low cost, and resistance to corrosion [5]. It is

well known that CO_2 can be reduced into fuels, e.g., CO, CH_4, CH_3OH, H_2, etc. by using TiO_2 as the photocatalyst under ultraviolet (UV) light illumination [6–9]. However, pure TiO_2 has the limitation. It is only active when irradiated by UV light, which is not effective under sunlight. Since the solar spectrum only consists of about 4% of UV light, sunlight is not able to active the TiO_2 effectively for photocatalytic reaction. In addition, TiO_2 has a high electron/hole pair recombination rate compared to the rate of chemical interaction with the absorbed species for redox reactions [10].

Recently, studies on CO_2 photochemical reduction by TiO_2 have been carried out from the viewpoint of performance promotion by extending absorption wavelength toward visible region. It was reported that a transition metal doping is useful technique for extending the absorbance of TiO_2 into the visible region [11–15]. Noble metal doping such as Pt, Pd, Au and Ag [11], Au, Pd-three dimensionally ordered macroporous TiO_2 [12], composition materials formed by GaP and TiO_2 [13], nanocomposite CdS/TiO_2 combining two different band gap photocatalysts [14], and carbon-based AgBr nanocomposited TiO_2 [15], had been attempted to overcome the shortcomings of the pure TiO_2. They could improve the CO_2 reduction performance; however, the concentrations in the products achieved in all the attempts so far were still low, ranging from 1 to 150 μmol/g-cat [11–16].

Though various metals have been used for doping [11–16], Cu is considered as a favorite candidate. Cu can extend the absorption band to 600–800 nm [17, 18], which covers the whole visible light range. Cu-decorated TiO_2 nanorod thin film performed 10 times yield as large as TiO_2 for C_2H_5OH production [19]. Cu-loaded N/TiO_2 also showed the good performance which yielded eight times as large as TiO_2 for CH_4 production [20]. Noble metals such as Pt and Au are too expensive to be used in industrial scale. Therefore, Cu is the best candidate because of its high efficiency and low cost compared to noble metals. Due to its availability as well as above described characteristics, Cu is selected as the dopant in this study.

Since a reductant is necessary for CO_2 reduction to produce fuel; H_2O and H_2 are usually used as reductants according to the review papers [7, 9]. To promote the CO_2 reduction performance of photocatalyst, it is important to select the optimum reductant which provides the proton (H^+) for the reaction scheme of CO_2 reduction with H_2O is as follows [21–23]:

<Photocatalytic reaction>

$$TiO_2 + h\nu \rightarrow h^+ + e^- \quad (1)$$

<Oxidization>

$$H_2O + h^+ \rightarrow \cdot OH + H^+ \quad (2)$$

$$\cdot OH + H_2O + h^+ \rightarrow O_2 + 3H^+ \quad (3)$$

<Reduction>

$$CO_2 + 2H^+ + 2e^- \rightarrow CO + H_2O \quad (4)$$

$$CO + 8H^+ + 8e^- \rightarrow CH_4 \quad (5)$$

The reaction scheme of CO_2 reduction with H_2 is as follows [24]:

<Photocatalytic reaction>

$$TiO_2 + h\nu \rightarrow h^+ + e^- \quad (6)$$

<Oxidization>

$$H_2 + 2h^+ \rightarrow 2H^+ + 2e^- \quad (7)$$

<Reduction>

$$CO_2 + e^- \rightarrow \cdot CO_2^- \quad (8)$$

$$\cdot CO_2^- + H^+ + e^- \rightarrow HCOO^- \quad (9)$$

$$HCOO^- + H^+ \rightarrow CO + H_2O \quad (10)$$

$$H^+ + e^- \rightarrow \cdot H \quad (11)$$

$$CO_2 + 8e^- + 8 \cdot H \rightarrow CH_4 + 2H_2O \quad (12)$$

The reaction scheme to reduce CO_2 with NH_3 can be summarized as shown below [24, 25]:

<Photocatalytic reaction>

$$TiO_2 + h\nu \rightarrow h^+ + e^- \quad (13)$$

<Oxidization>

$$2NH_3 \rightarrow N_2 + 3H_2 \quad (14)$$

$$H_2 \rightarrow 2H^+ + 2e^- \quad (15)$$

<Reduction>

$$H^+ + e^- \rightarrow \cdot H \quad (16)$$

$$CO_2 + e^- \rightarrow \cdot CO_2^- \quad (17)$$

$$\cdot CO_2^- + H^+ + e^- \rightarrow HCOO^- \quad (18)$$

$$HCOO^- + H^+ \rightarrow CO + H_2O \quad (19)$$

$$CO_2 + 8H^+ + 8e^- \rightarrow CH_4 + 2H_2O \quad (20)$$

There are some reports on CO_2 reduction with either H_2O or H_2 [7, 9]. However, the effect of using H_2O and H_2 or NH_3 together as reductants is not investigated well. Though a few studies using pure TiO_2 under $CO_2/H_2/H_2O$ condition were reported [24, 26], the effect of ratio of CO_2, H_2 and H_2O or NH_3 as well as the effect of Cu doping with TiO_2 on CO_2 reduction performance of photocatalyst were not investigated previously.

Consequently, the purpose of this chapter is to clarify the effect of molar ratio of CO_2 to H_2O and H_2 or NH_3 on the performance of CO_2 reduction with Cu/TiO_2. The CO_2 reduction performance with H_2O and H_2 or NH_3 using Cu/TiO_2 coated on netlike glass fiber as photocatalyst under the condition of illuminating Xe lamp with or without UV light was investigated. Cu is loaded on TiO_2-coated netlike glass fiber by pulse arc plasma method which can emit nanosized Cu particles by applying high electron potential difference. The amount of loaded Cu can be controlled by the pulse number. Cu/TiO_2 prepared was characterized by Scanning Electron Microscope (SEM) and Electron Probe Micro Analyzer (EPMA), Transmission Electron Microscope (TEM), Energy Dispersive X-ray Spectrometry (EDX), and Electron Energy Loss Spectrum (EELS) analysis. The CO_2 reduction performance with H_2O and H_2 or NH_3 under the condition of illuminating Xe lamp with or without UV

light was investigated. The molar ratio of $CO_2/H_2/H_2O$ was changed for 1:1:1, 1:0.5:1, 1:1:0.5, 1:0.5:0.5 to clarify the optimum combination of $CO_2/H_2/H_2O$ for CO_2 reduction with Cu/TiO_2. According to the reaction scheme to reduce CO_2 with H_2O or NH_3 as shown above, the theoretical molar ratio of CO_2/H_2O to produce CO or CH_4 is 1:1 or 1:4, respectively, while that of CO_2/NH_3 to produce CO or CH_4 is 3:2, 3:8, respectively. Therefore, this study assumes that the molar ratio of $CO_2/NH_3/H_2O$ = 3:2:3 and 3:8:12 are theoretical molar ratio to produce CO and CH_4, respectively. Moreover, the effect of overlapping two layers of Cu/TiO_2-coated netlike glass fiber on CO_2 reduction performance with H_2 and H_2O was investigated.

2. Experiment

2.1 Preparation of Cu/TiO_2 film

The combination of sol–gel and dip-coating process was used for preparing TiO_2 film. TiO_2 sol solution was made by mixing $[(CH_3)_2CHO]_4Ti$ (purity of 95 wt%, Nacalai Tesque Co.) of 0.3 mol, anhydrous C_2H_5OH (purity of 99.5 wt%, Nacalai Tesque Co.) of 2.4 mol, distilled water of 0.3 mol, and HCl (purity of 35 wt%, Nacalai Tesque Co.) of 0.1 mol. Netlike glass fiber was cut like a disc, and its diameter and thickness were 50 mm and 1 mm, respectively. The netlike glass fiber disc was dipped into TiO_2 sol solution at the speed of 1.5 mm/s and pulled up at the fixed speed of 0.2 mm/s. Then, it was dried out and fired under the controlled firing temperature (*FT*) and firing duration time (*FD*), resulting that TiO_2 film was fastened on the netlike glass fiber. *FT* and *FD* were set at 623 K and 180 s, respectively. Cu was loaded on TiO_2 film by pulse arc plasma method. The pulse arc plasma gun device (ULVAC, Inc., ARL-300) having Cu electrode whose diameter was 10 mm was applied for Cu loading. After the netlike glass fiber coated with TiO_2 was set in chamber of the pulse arc plasma gun device which was vacuumed, the nanosized Cu particles were emitted from Cu electrode with applying the electrical potential difference of 200 V. The pulse arc plasma gun can evaporate Cu particle over the target in the circle area whose diameter is 100 mm when the distance between Cu electrode and the target is 160 mm. Since the difference between Cu electrode and TiO_2 film was 150 nm in the present study, Cu particle can be evaporated over TiO_2 film uniformly. The amount of loaded Cu was controlled by the pulse number. In the present study, the pulse number was set at 100. Since the netlike glass fiber is transparent, the light can pass through the netlike glass fiber. The present study has also investigated if two layers of two Cu/TiO_2 coated on netlike glass fiber put on the top of the other (with certain distance, i.e., overlapping), what impact/improvement would be on the CO_2 reduction performance. The overlapping two layers of Cu/TiO_2 coated on netlike glass fiber is expected to utilize the light effectively as well as to increase the amount of photocatalyst used for CO_2 reduction.

2.2 Characterization of Cu/TiO_2 film

The structure and crystallization characteristics of Cu/TiO_2 film were evaluated by SEM (JXS-8530F, JEOL Ltd.), EPMA (JXA-8530F, JEOL Ltd.), TEM (JEM-2100/HK, JEOL Ltd.), EDX (JEM-2100F/HK, JEOL Ltd.), and EELS (JEM-ARM2007 Cold, JEOL Ltd.). Since these measurement instruments use electron for analysis, the sample should be an electron conductor. Since netlike glass disc was not an electron for analysis, the carbon vapor deposition was conducted by the dedicated device (JEE-420, JEOL Ltd.) for Cu/TiO_2 coated on netlike glass disc before analysis. The thickness of carbon deposited on sample was approximately 20–30 nm.

The electron probe emits the electrons to the sample under the acceleration voltage of 15 kV and the current of 3.0×10^{-8} A, when the surface structure of sample is analyzed by SEM. The characteristic X-ray is detected by EPMA at the same time, resulting that the concentration of channel element is analyzed according to the relationship between the characteristic X-ray energy and the atomic number. The spatial resolutions of SEM and EPMA are 10 μm. The EPMA analysis helps not only to understand the coating state of prepared photocatalyst but also to measure the amount of doped metal within TiO_2 film on the base material.

The electron probe emits the electron to the sample under the acceleration voltage of 200 kV, when the inner structure of sample is analyzed by TEM. The size, thickness, and structure of loaded Cu were evaluated. The characteristic X-ray is detected by EDX at the same time, resulting that the concentration distribution of chemical element toward thickness direction of the sample is analyzed. In the present study, the concentration distribution of Ti and Cu were analyzed.

EELS can be applied not only for element detection but also determination of oxidization states of some transition metals. The EELS characterization was performed by JEM-ARM200F equipped with GIF Quantum having 2048 ch. The dispersion of 0.5 eV/ch can be achieved for the full width at half maximum of the zero loss peak.

2.3 CO_2 reduction experiment

Figure 1 [27, 28] shows the experimental set-up of the reactor composing of stainless tube (100 mm (*H.*) × 50 mm (*I.D.*)), Cu/TiO_2 film coated on netlike glass disc (50 mm (*D.*) × 1 mm (*t.*)) located on the Teflon cylinder (50 mm (*H.*) × 50 mm (*D.*)), a quartz glass disc (84 mm (*D.*) × 10 mm (*t.*)), a sharp cut filter cutting off the light whose wavelength is below 400 nm (SCF-49.5C-42 L, SIGMA KOKI CO. LTD.), a 150 W Xe lamp (L2175, Hamamatsu Photonics K. K.), mass flow controller, and CO_2 gas cylinder. The volume of reactor to charge CO_2 is 1.3×10^{-4} m^3. The light of Xe lamp which is located inside the stainless tube illuminates Cu/TiO_2 film coated on the netlike glass disc through the sharp cut filter and the quartz glass disc that are at the top of the stainless tube. The wavelength of light from Xe lamp is ranged from 185 to 2000 nm. Since the sharp cut filter can remove UV components of the light from the Xe lamp, the wavelength of light from Xe lamp is ranged from 401 to 2000 nm with the filter. **Figure 2** [29] shows the performance of the sharp cut filter to cut off the wavelength is below 400 nm. The

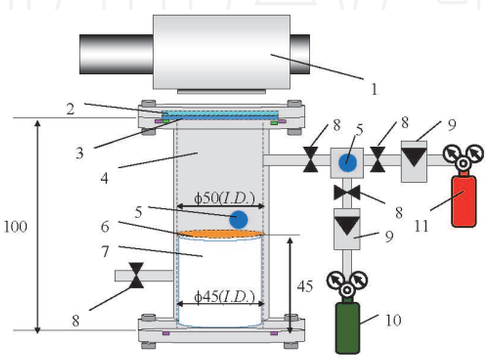

1. Xe lamp, 2. Sharp cut filter, 3. Quartz glass disc, 4. Stainless pipe,
5. Gas sampling tap, 6. Photocatalyst, 7. Teflon cylinder, 8. Valve,
9. Mass flow controller, 10. CO_2 gas cylinder (99.995 vol%),
11. H_2 gas cylinder (99.99999 vol%)

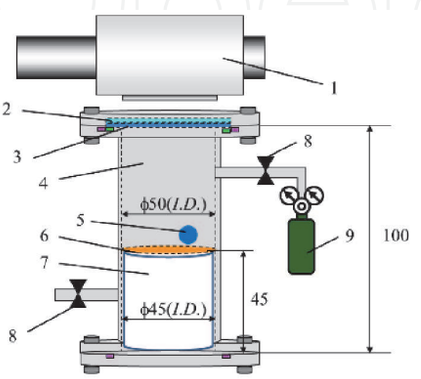

1. Xe lamp, 2. Sharp cut filter, 3. Quartz glass disc, 4. Stainless tube,
5. Gas sampling tap, 6. Photocatalyst, 7. Teflon cylinder, 8. Valve,
9. CO_2 gas cylinder (99.995 vol%)

Figure 1.
Schematic drawing of CO_2 reduction experimental set-up (left: $CO_2/H_2/H_2O$ system; right: $CO_2/NH_3/H_2O$ system).

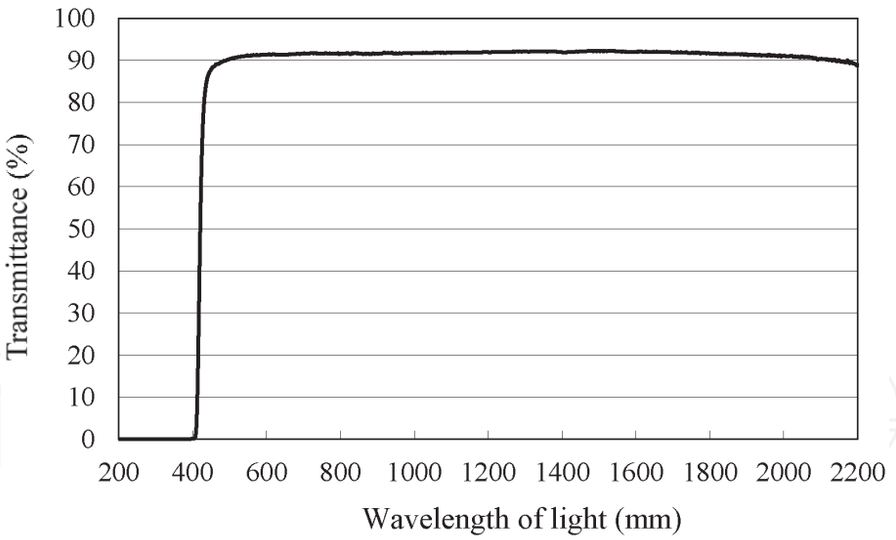

Figure 2.
Light transmittance data of sharp cut filter.

average light intensity of Xe lamp without and with the sharp cut filter is 58.2 and 33.8 mW/cm^2, respectively.

In the CO_2 reduction experiment with H_2 and H_2O, CO_2 gas with the purity of 99.9 vol% which were controlled by mass flow controller was mixed in the buffer chamber and introduced into the reactor which was pre-vacuumed by a vacuum pump. The mixing ratio of CO_2 and H_2 was confirmed by TCD gas chromatograph (Micro GC CP4900, GL Science) before introducing into the reactor. After confirming the mixing ratio of CO_2 and H_2, the distilled water was injected into the reactor through a gas sampling tap by syringe and Xe lamp illumination was turned on the same time. The amount of injected water was measured and controlled by the syringe. The injected water vaporized completely in the reactor. The molar ratio of $CO_2/H_2/H_2O$ was set at 1:1:1, 1:0.5:1, 1:1:0.5, 1:0.5:0.5. Due to the heat of Xe lamp, the temperature in reactor was attained at 343 K within an hour and kept an approximately 343 K during the experiment.

In the CO_2 reduction experiment with NH_3 and H_2O, after purging the reactor with CO_2 gas of 99.9 vol% purity introduced in the reactor, which was pre-vacuumed by a vacuum pump, for 15 minutes, the valves located at the inlet and the outlet of reactor were closed. After confirming the pressure and gas temperature in the reactor at 0.1 MPa and 298 K, respectively, the NH_3 aqueous solution (NH_3; 50 vol%), which was changed according to the planed molar ratio, was injected into the reactor through gas sampling tap, and Xe lamp illumination was turned on the same time. The NH_3 aqueous solution injected was vaporized completely in the reactor. Due to the heat of Xe lamp, the temperature in the reactor was attained at 343 K within an hour and kept at approximately 343 K during the experiment. The molar ratio of $CO_2/NH_3/H_2O$ was set at 1:1:1, 1:0.5:1, 1:1:0.5, 1:0.5:0.5, 3:2:3, 3:8:12, respectively. The gas in the reactor was sampled every 24 hours during the experiment. The gas samples were analyzed by FID gas chromatograph (GC353B, GL Science). Minimum resolution of FID gas chromatograph and methanizer is 1 ppmV.

3. Results and discussion

3.1 Characterization analysis of Cu/TiO_2 film

Figure 3 shows SEM image of Cu/TiO_2 film coated on netlike glass disc [28]. The SEM image was taken at 1500 times magnification. **Figure 4** shows EPMA image of

Cu/TiO_2 film coated on netlike glass disc [28]. EPMA analysis was carried out for SEM images taken by 1500 times magnification. In EPMA image, the concentration of each element in observation area is indicated by the different colors. Light colors, for example, white, pink, and red indicate that the amount of element is large, while dark colors like black and blue indicate that the amount of element is small.

From these figures, it can be observed that TiO_2 film was coated on netlike glass fiber. During firing process, the temperature profile of TiO_2 solution adhered on the netlike glass disc was not even due to the different thermal conductivities of Ti and SiO_2. Their thermal conductivities of Ti and SiO_2 at 600 K are 19.4 and 1.8 W/(m·K) [30], respectively. Due to thermal expansion and shrinkage around netlike glass fiber, it can be considered that thermal crack is formed on the TiO_2 film.

In addition, it is observed from **Figure 4** that nanosized Cu particles are loaded on TiO_2 uniformly, resulted from that the pulse arc plasma method can emit nanosized Cu particles.

To evaluate the amount of loaded Cu within TiO_2 film quantitatively, the observation area, which is the center of netlike glass disc, of diameter of 300 μm is analyzed by EPMA. The ratio of Cu to Ti is counted by averaging the data obtained in this area. As a result, the weight percentages of elements of Cu and Ti in the Cu/TiO_2 film are 0.6 and 99.4 wt%, respectively.

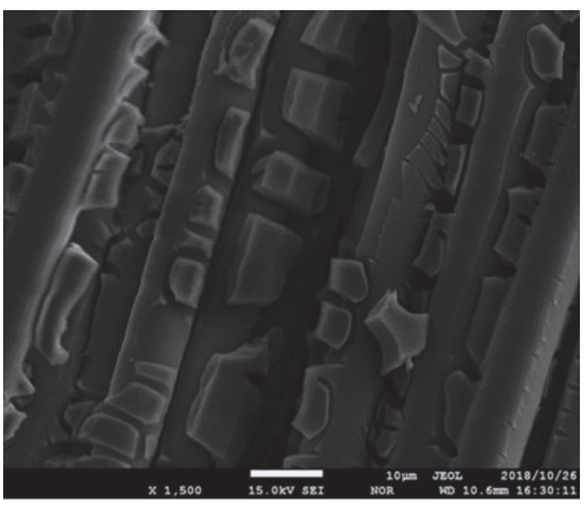

Figure 3.
SEM image of Cu/TiO_2 film coated on netlike glass disc.

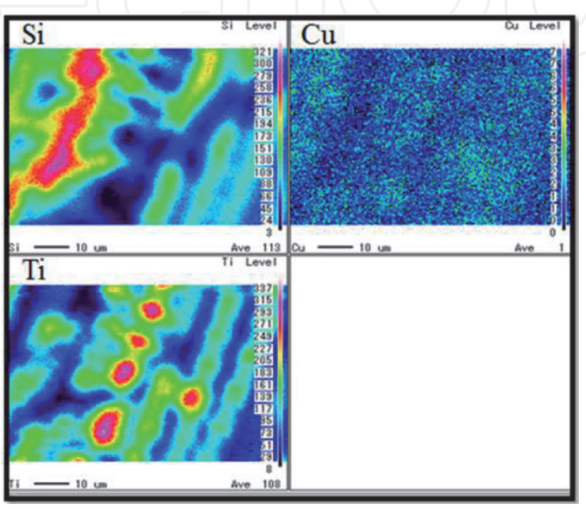

Figure 4.
EPMA image of Cu/TiO_2 film coated on netlike glass disc.

Figures 5 and **6** show TEM and EDX images of Cu/TiO_2 film, respectively [27]. ESX analysis was carried out using TEM image taken by 150,000 times magnification. According to **Figure 6**, it is observed that Cu particles are distributed in TiO_2 film. Though many Cu particles are loaded on the upside of TiO_2 film, it is not confirmed that the Cu layer is formed.

Figure 7 shows EELS spectra of Cu in Cu/TiO_2 film [27]. From this figure, the peaks at around 932 and 952 eV can be observed. Compared to the report investigating peaks of Cu, Cu_2O, and CuO [31], the EELS spectra of Cu_2O matches with **Figure 7**. Therefore, Cu in Cu/TiO_2 prepared in this study exists as Cu^+ ion in Cu_2O. It was reported that the heterojunctions between CuO and TiO_2 contributed to the promotion of the photoactivity [32]. In addition, it was reported that Cu^+ was more active than Cu^{2+} [33]. Therefore, it is expected that Cu^+ would play a role to enhance the CO_2 reduction performance in this study. **Figure 8** shows EELS spectra of TiO_2 referred from EELS data base [34]. Comparing **Figure 8** with **Figure 7**, EELS spectra of TiO_2 is very different from EELS spectra of Cu in Cu/TiO_2.

3.2 Effect of molar ratio of CO_2, H_2, and H_2O on CO_2 reduction characteristics

Figures 9 and **10** show the concentration changes of CO and CH_4 produced in the reactor along the time under the illumination of Xe lamp with UV light,

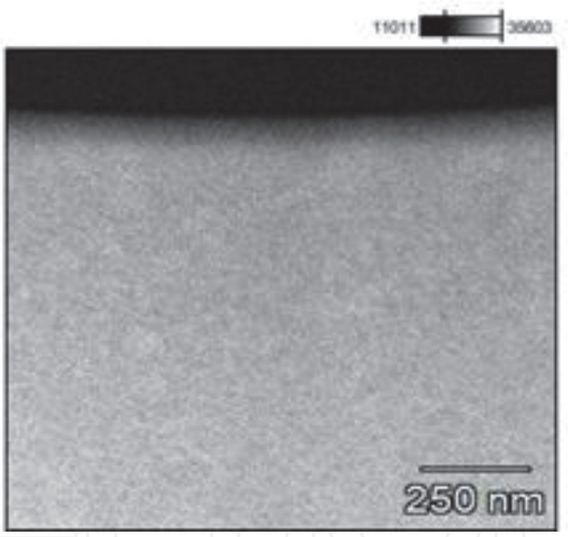

Figure 5.
TEM image of Cu/TiO_2 film.

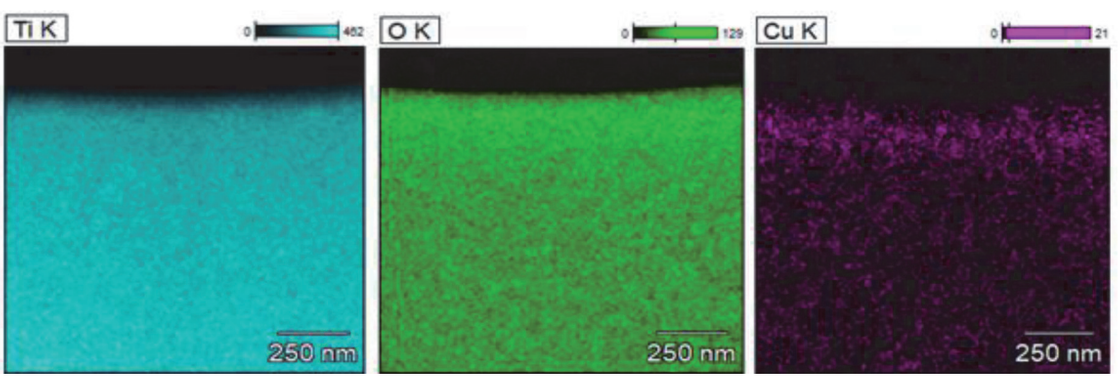

Figure 6.
EDX images of Cu/TiO_2 film.

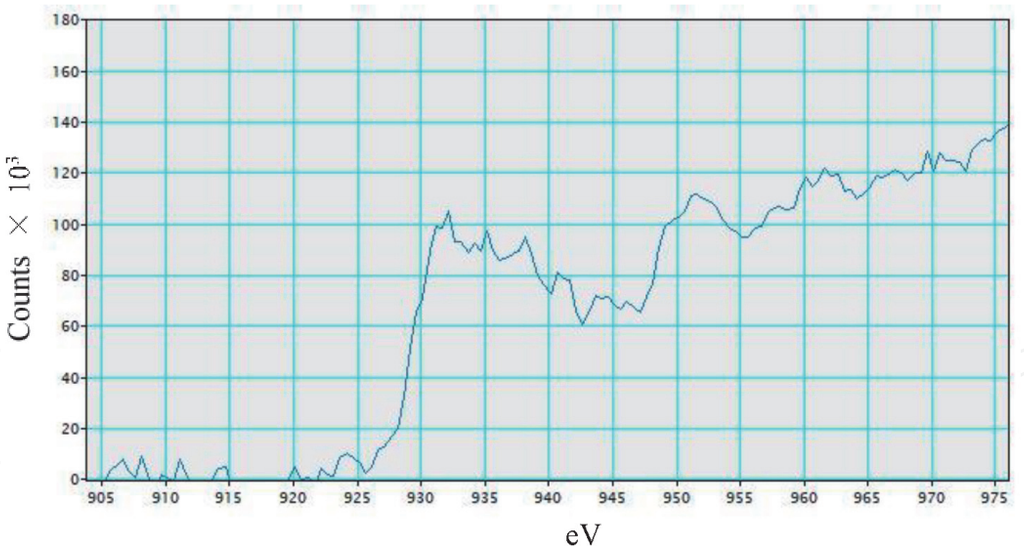

Figure 7.
EELS spectra of Cu in Cu/TiO_2.

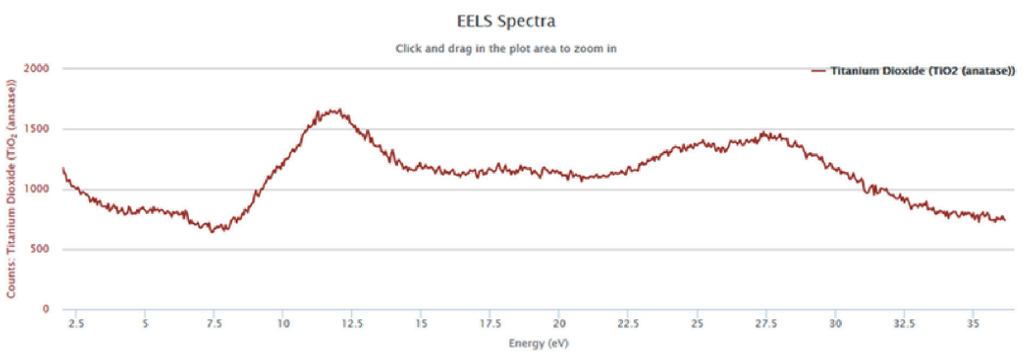

Figure 8.
EELS spectra of TiO_2 referred from EELS data base [34].

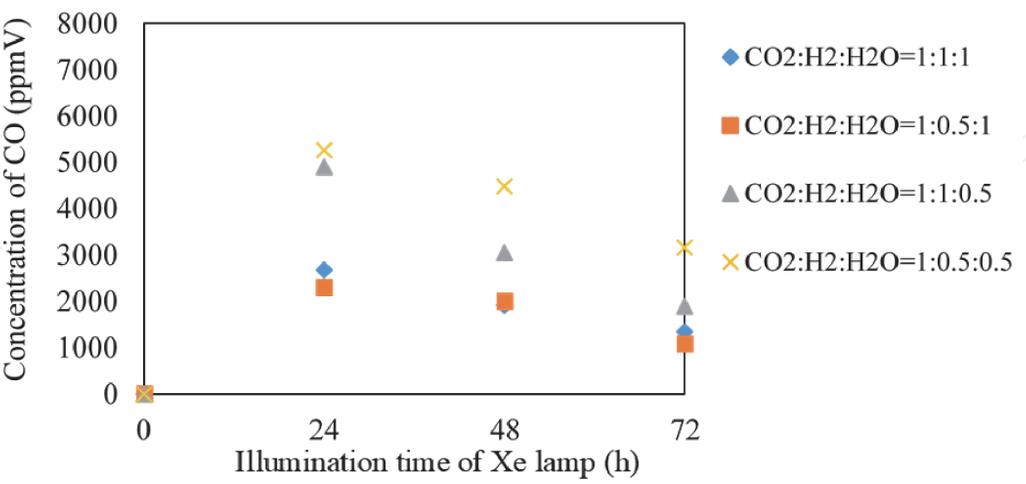

Figure 9.
Change of concentration of CO with time for several molar ratios of $CO_2/H_2/H_2O$ under illumination condition with UV light.

respectively. **Figures 11** and **12** show the molar quantities of CO and CH_4 per weight of photocatalyst in the reactor along the time under the illumination of Xe lamp with UV light, respectively. The amount of Cu/TiO_2 is 0.2 g. In this experiment, a blank test, that was running the same experiment without illumination of Xe lamp,

had been carried out to set up a reference case. No fuel was produced in the blank test as expected.

According to **Figures 9–12**, the CO_2 reduction performance is the highest for the molar ratio of $CO_2/H_2/H_2O$ = 1:0.5:0.5. Since the reaction scheme of $CO_2/H_2/H_2O$ is not fully understood, this study refers to the reaction scheme of CO_2/H_2O and CO_2/H_2 as shown by Eqs. (1)–(12). It is known from the reaction scheme that the theoretical molar ratio of CO_2/H_2O and CO_2/H_2 to produce CO is 1:1. On the other hand, the theoretical molar ratio of CO_2/H_2O and CO_2/H_2 to produce CO is 1:4. Since the molar ratio of $CO_2/H_2/H_2O$ = 1:0.5:0.5 can be regarded as the molar ratio of CO_2/total reductants = 1:1, it is believed that the results of this study follow the reaction scheme presented in Eqs. (1)–(12). Comparing the CO production with the CH_4 production, CO is produced first. According to Eq. (5), it is believed that some CO might be converted into CH_4. Therefore, the start of CH_4 production is slower than that of CO production. Producing CH_4 needs four times H^+ and electrons as many as producing CO needs. Therefore, it is revealed that the optimum molar ratio

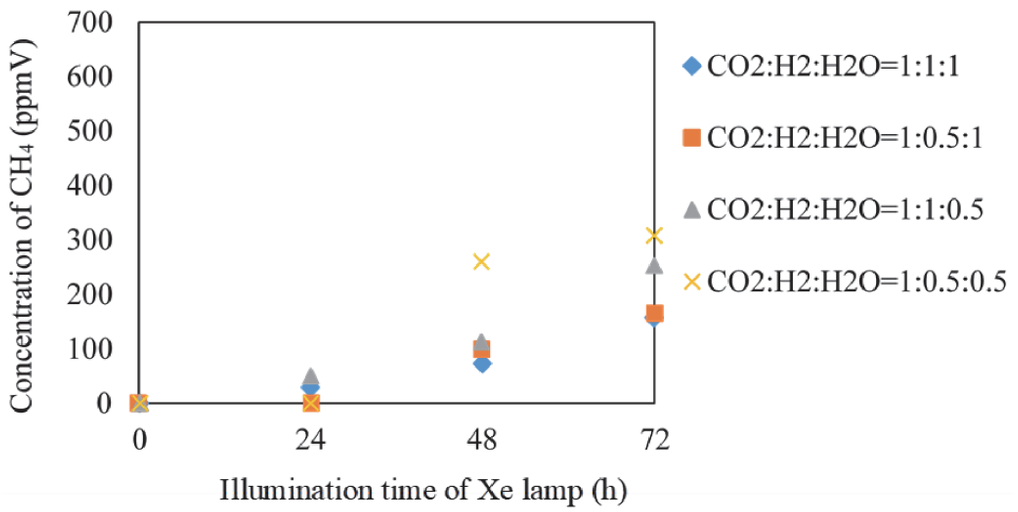

Figure 10.
Change of concentration of CH_4 with time for several molar ratios of $CO_2/H_2/H_2O$ under illumination condition with UV light.

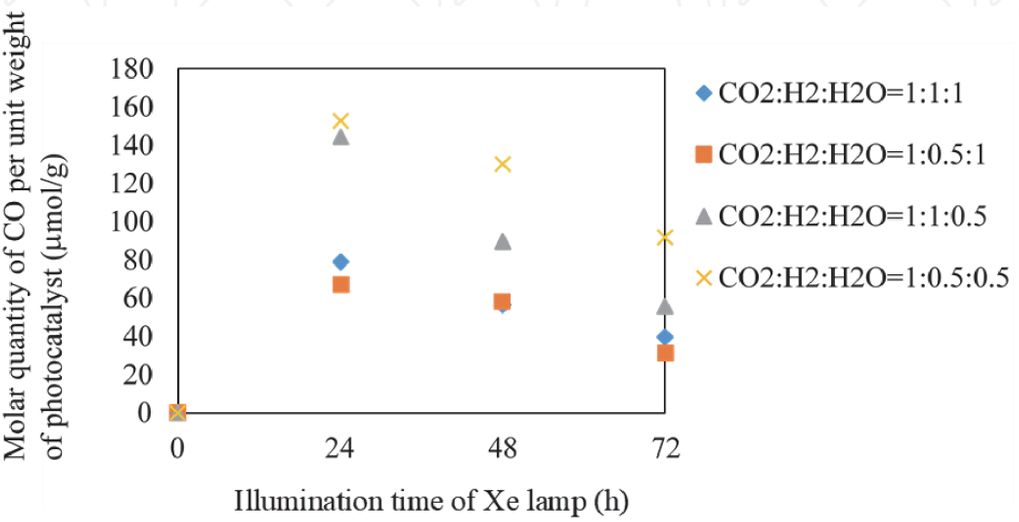

Figure 11.
Change of molar quantity of CO per unit weight of photocatalyst with time for several molar ratios of $CO_2/H_2/H_2O$ under illumination condition with UV light.

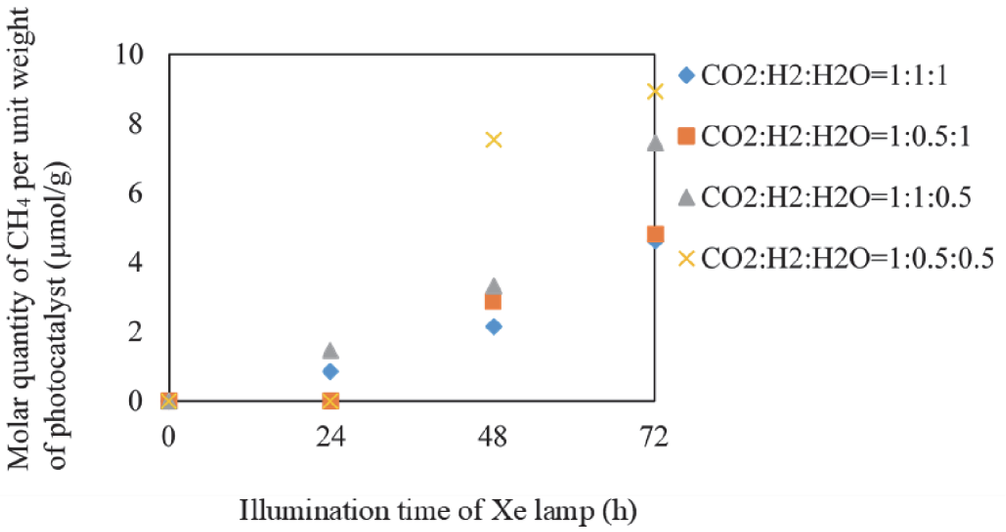

Figure 12.
Change of molar quantity of CH_4 per unit weight of photocatalyst with time for several molar ratios of $CO_2/H_2/H_2O$ under illumination condition with UV light.

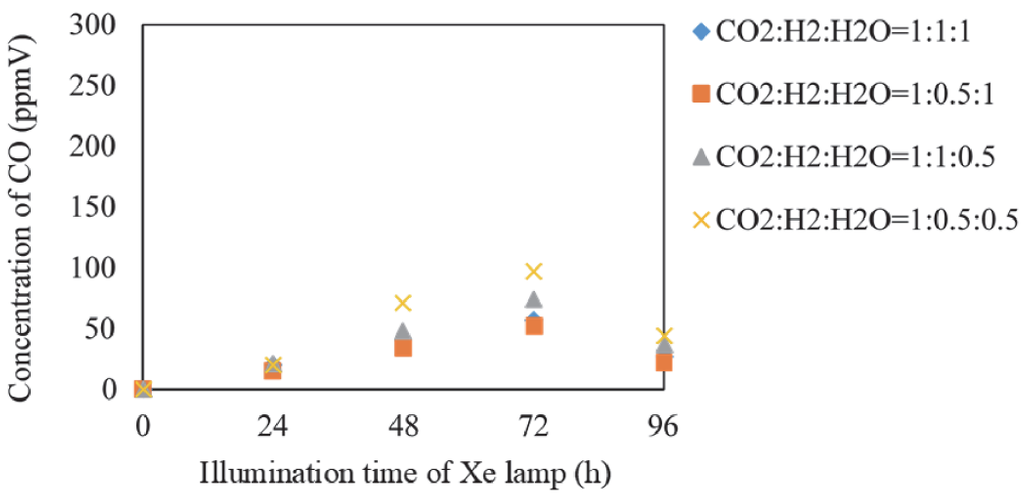

Figure 13.
Change of concentration of CO with time for several molar ratios of $CO_2/H_2/H_2O$ under illumination condition without UV light.

of $CO_2/H_2/H_2O$ is decided by the CO production scheme. Though CO decreases after reaching the peak, CH_4 increases gradually.

According to Hinojosa-Reyes et al. [35], TiO_2 and Cu_2O formation leads to the photocatalytic activity since Cu_2O is a semiconductor with small band gap energy. In addition, Cu performs to avoid the electron and hole recombination and promotes the charge transfer. In this study, it seems that the effect of Cu and Cu_2O on photoactivity is performed.

Figures 13 and **14** show the concentration changes of CO produced and the molar quantity of CO per weight of photocatalyst in the reactor under the illumination of Xe lamp without UV light, respectively. In this experiment, CO is the only fuel produced from the reactions.

According to **Figures 13** and **14**, the CO_2 reduction performance is also the highest for the molar ratio of $CO_2/H_2/H_2O$ = 1:0.5:0.5 in this case. It is considered that the same reaction mechanism as mentioned above is conducted. The CO_2 reduction performance of Cu/TiO_2 under the illumination condition without UV

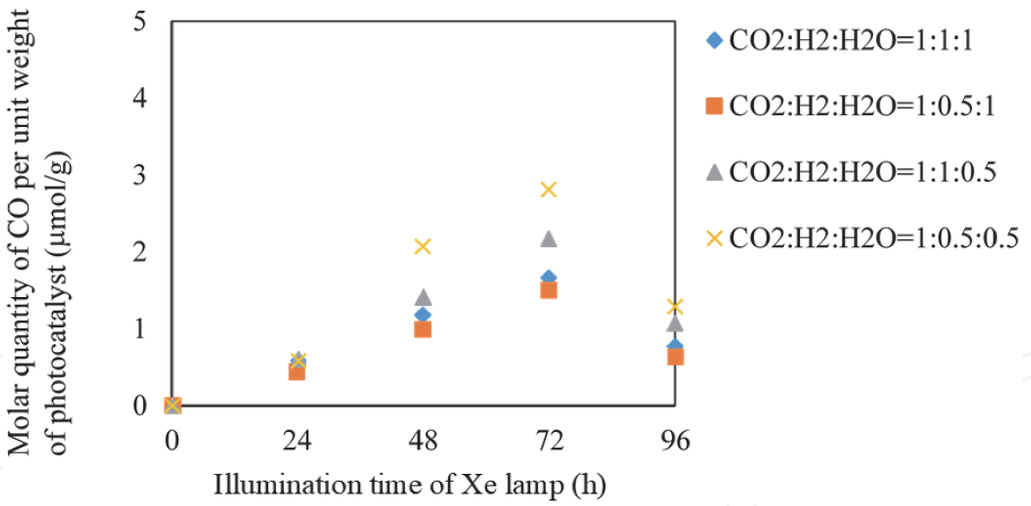

Figure 14.
Change of molar quantity of CO per unit weight of photocatalyst with time for several molar ratios of $CO_2/H_2/H_2O$ under illumination condition without UV light.

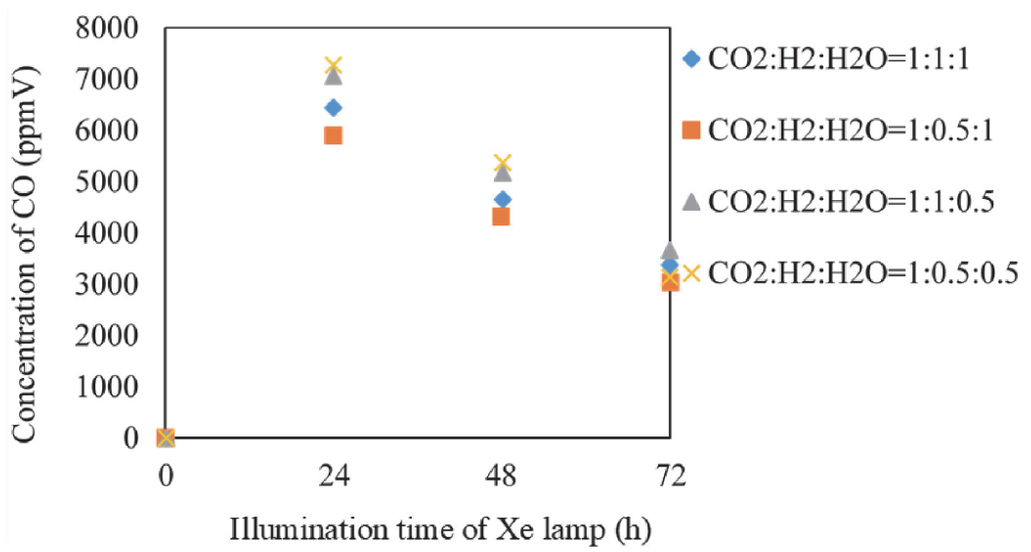

Figure 15.
Change of concentration of CO for Cu/TiO_2 overlapped with time for several molar ratios of $CO_2/H_2/H_2O$ under illumination condition with UV light.

light is lower than that under the illumination condition with UV light. Therefore, it can be claimed that Cu/TiO_2 obtains the main photoenergy from UV light.

3.3 Effect of overlapping of Cu/TiO_2 film with H_2 and H_2O on CO_2 reduction characteristics

Figures 15 and **16** show the concentration change of CO and CH_4 produced in the reactor under the illumination of Xe lamp with UV light, with two Cu/TiO_2 films coated on netlike glass discs overlapped, respectively. The photocatalyst is coated on both upper and lower surfaces of the top disc and only the upper surface of the bottom disc.

Figures 17 and **18** show the molar quantities of CO and CH_4 per weight of photocatalyst in the reactor along the time under the Xe lamp with UV light, respectively. The total amount of Cu/TiO_2 on two discs is 0.4 g.

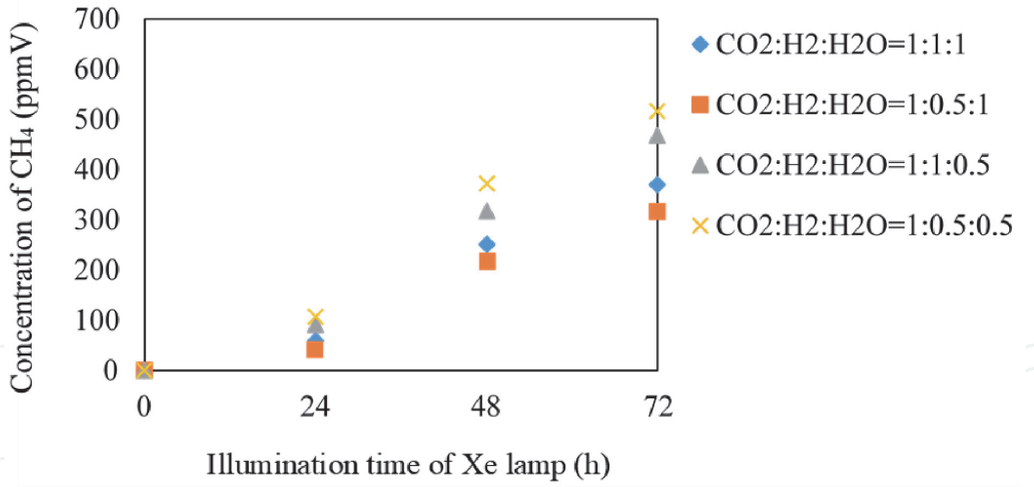

Figure 16.
Change of concentration of CH_4 for Cu/TiO_2 overlapped with time for several molar ratios of $CO_2/H_2/H_2O$ under illumination condition with UV light.

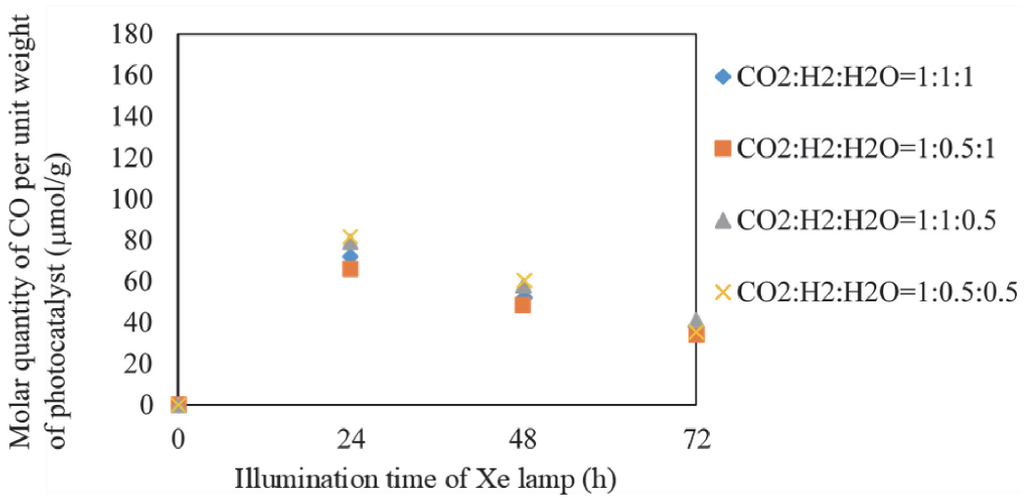

Figure 17.
Change of molar quantity of CO per unit weight of photocatalyst for Cu/TiO_2 overlapped with time for several molar ratios of $CO_2/H_2/H_2O$ under illumination condition with UV light.

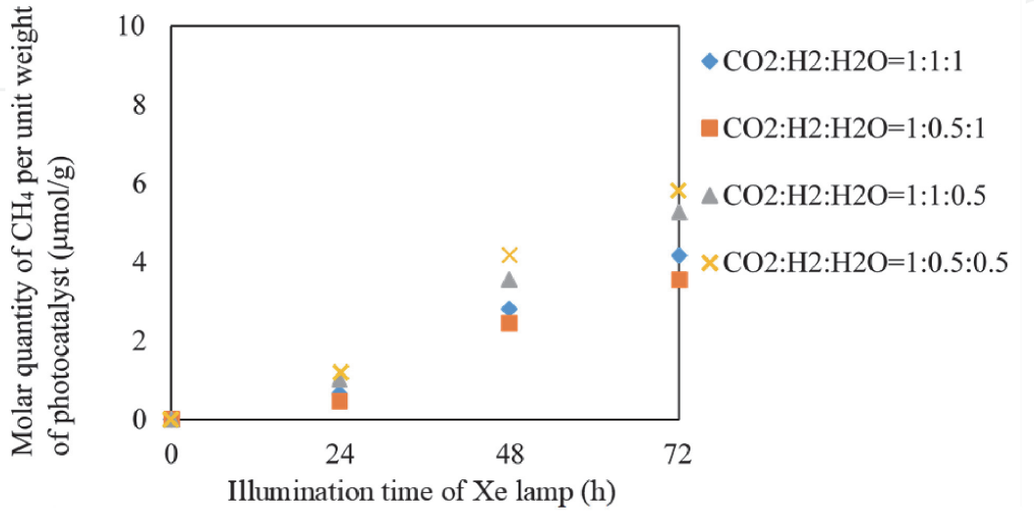

Figure 18.
Change of molar quantity of CH_4 per unit weight of photocatalyst for Cu/TiO_2 overlapped with time for several molar ratios of $CO_2/H_2/H_2O$ under illumination condition with UV light.

According to **Figures 15–18**, the CO_2 reduction performance is the highest for the molar ratio of $CO_2/H_2/H_2O$ = 1:0.5:0.5, the same as that in the case of single Cu/TiO_2 disc. In addition, the order of CO_2 reduction performance of Cu/TiO_2 overlapped is the same as that of single Cu/TiO_2. However, comparing **Figures 15** and **16** with **Figures 9** and **10**, the concentrations of CO and CH_4 for two Cu/TiO_2 discs overlapped are higher than those for single Cu/TiO_2 disc under every molar ratio of $CO_2/H_2/H_2O$. The highest concentration of CO for Cu/TiO_2 overlapped is 7273 ppmV, which is 1.4 times as large as that for single Cu/TiO_2. On the other hand, the highest concentration of CH_4 for Cu/TiO_2 overlapped is 516 ppmV, which is 1.7 times as large as that for single Cu/TiO_2. In the case of two discs overlapped, the following things are believed: (i) the amount of photocatalyst used for photocatalysis reaction is increased, (ii) the electron transfer between two Cu/TiO_2 films promotes the activity of photocatalysis reaction, and (iii) the lower positioned Cu/TiO_2 disc utilizes the light passing through the top disc.

However, comparing **Figures 17** and **18** with **Figures 11** and **12**, the molar quantities of CO and CH_4 per weight of photocatalyst in two discs case are lower than those for single Cu/TiO_2 disc case under every molar ratio of $CO_2/H_2/H_2O$. The highest molar quantity of CO per weight of photocatalyst in two discs overlapped case is 82 μmol/g, which is 54% of that in single disc case. Similarly, the highest molar quantity of CH_4 per weight of photocatalyst in two discs overlapped case is 5.8 μmol/g, which is 65% of that in single disc case. The reasons of this result are considered to be: (i) some parts of the Cu/TiO_2 film on the lower positioned disc cannot receive the light, (ii) if the produced fuel remains in the space between two discs, the reactants of CO_2, H_2, and H_2O would be blocked to reach the surface of photocatalyst, resulting that the photochemical reaction could not be carried out well even though the light is illuminated for photocatalyst.

Figures 19 and **20** show the concentration changes of CO produced and the molar quantity of CO per weight of photocatalyst in the reactor with two overlapped Cu/TiO_2 film coated on netlike glass disc under the illumination of Xe lamp without UV light, respectively. In this experiment, CO is the only produced from the reactions.

According to **Figures 19** and **20**, the CO_2 reduction performance in two discs case is the highest for the molar ratio of $CO_2/H_2/H_2O$ = 1:0.5:0.5 which is the same as

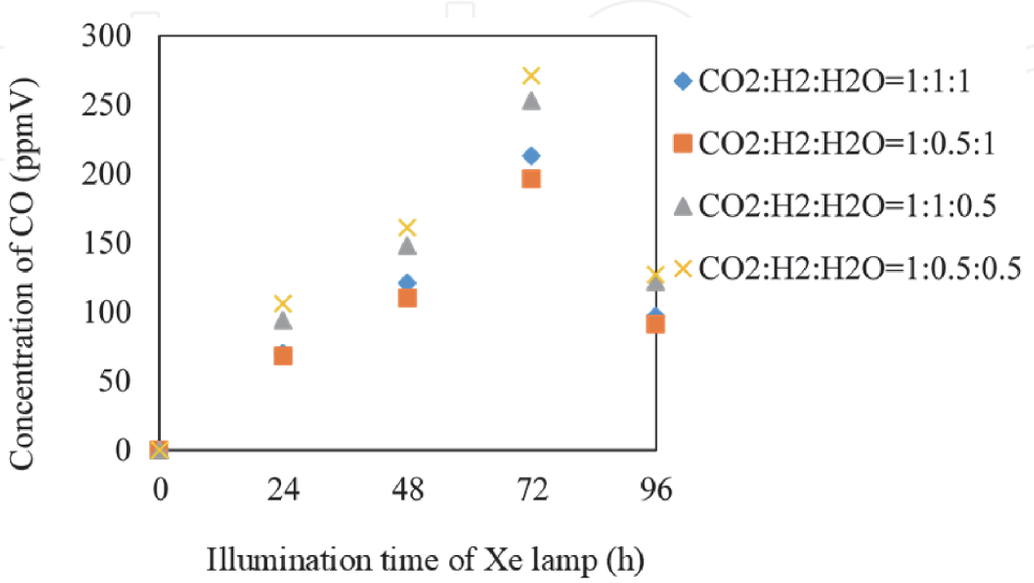

Figure 19.
Change of concentration of CO for Cu/TiO_2 overlapped with time for several molar ratios of $CO_2/H_2/H_2O$ under illumination condition without UV light.

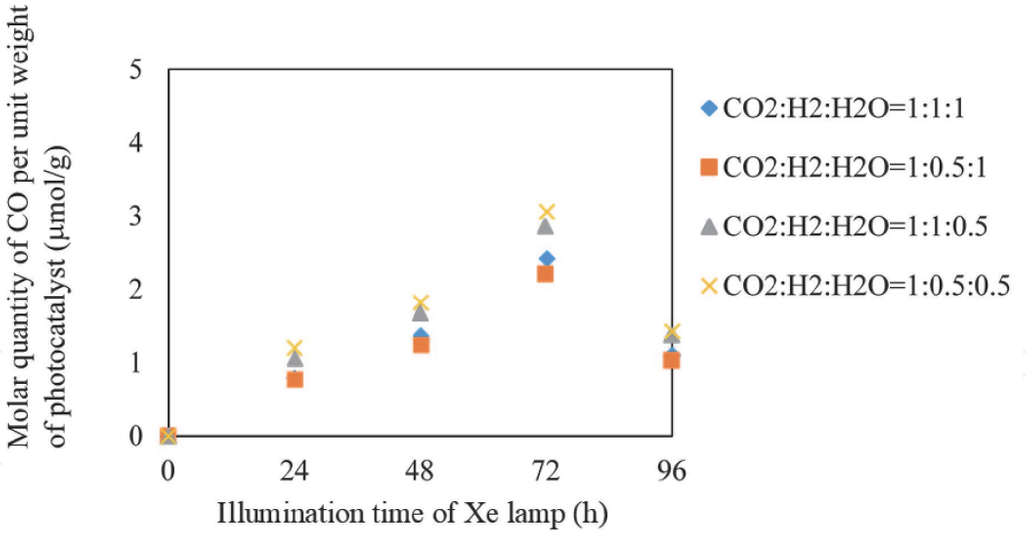

Figure 20.
Change of molar quantity of CO per unit weight of photocatalyst for Cu/TiO_2 overlapped with time for several molar ratios of $CO_2/H_2/H_2O$ under illumination condition without UV light.

that in the single disc case. The order of CO_2 reduction performance in two discs is the same as that in the single disc case. However, comparing **Figure 19** with **Figure 13**, the concentrations in two discs case are higher than those in single case under every molar ratio of $CO_2/H_2/H_2O$. The highest concentration of CO in two discs case is 271 ppmV, which is 2.8 times as large as that in single disc case. The same reasons explained in the case of illumination with UV light can be thought to cause the results.

In addition, comparing **Figure 20** with **Figure 14**, the molar quantity of CO per weight of photocatalyst in two Cu/TiO_2 discs overlapped case is singly higher than that in the single disc case under every molar ratio of $CO_2/H_2/H_2O$. The highest molar quantity of CO per weight of photocatalyst is 3.1 μmol/g in two disc cases, which is 1.1 times as large at that in the single disc case. Though the effect of overlapping layout is not obtained under the illumination condition with UV light, the effect of overlapping layout is confirmed under the illumination condition without UV light. Since the photochemical reaction rate and the amount of produced fuel are small under the no-UV illumination condition compared to that with UV light, it would be beneficial to the mass transfer between produced fuels and reactants of CO_2, H_2, and H_2O on the surface of photocatalyst in no-UV cases [36]. As a result, the mass transfer and photochemical reaction are carried out effectively in no-UV cases. Therefore, the effect of overlapping layout is obtained in no-UV cases. According to the previous reports [37, 38], the mass transfer is an inhibition factor to promote the CO_2 reduction performance of photocatalyst, and it is necessary to control the mass transfer rate to meet the photochemical reaction rate. **Figure 21** illustrates the comparison of mass and electron transfer within overlapped two photocatalysts in UV and no-UV illumination cases [27].

3.4 Effect of molar ratio of CO_2, NH_3 and H_2O on CO_2 reduction characteristics

Figures 22 and **23** show the concentration changes of formed CO and CH_4, along the time under the Xe lamp with UV light, respectively. The amount of Cu/TiO_2 on the netlike glass disc is 0.1 g. Before the experiments, a blank test, which was running the same experiment without illumination of Xe lamp, had been carried out to set up a reference case. No fuel was produced in the blank test as expected.

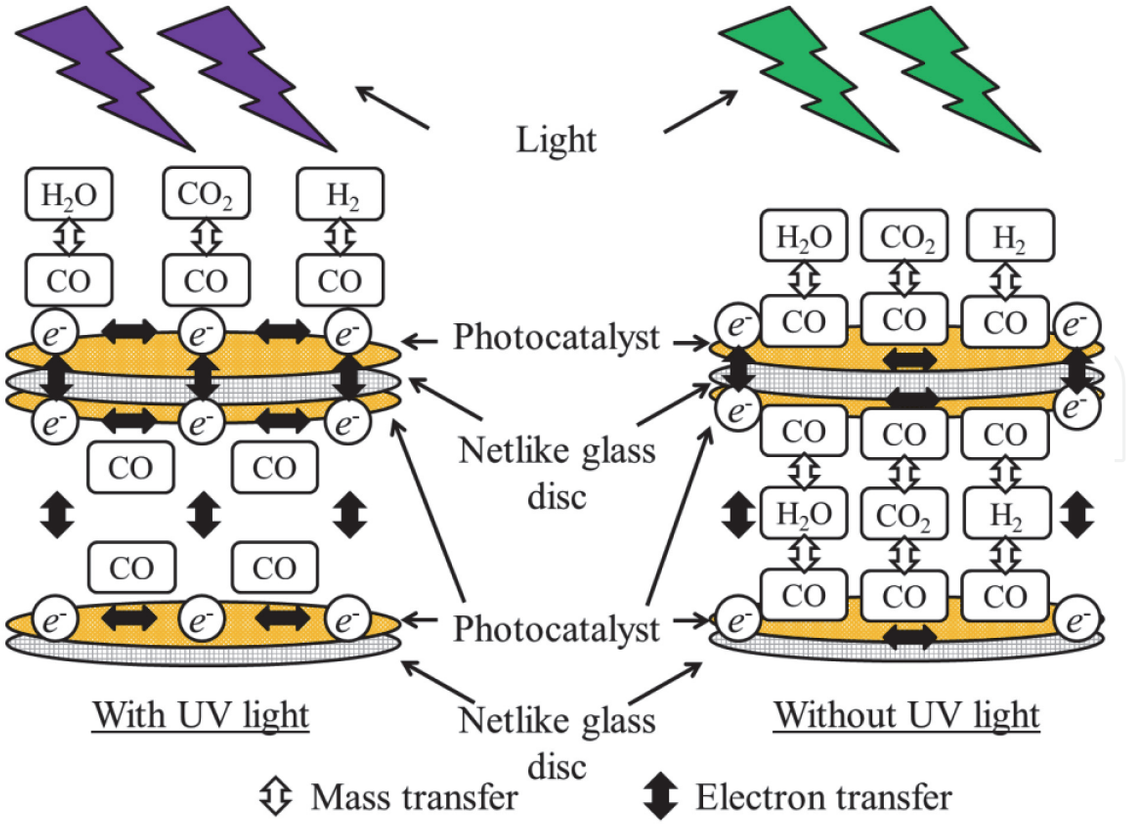

Figure 21.
Comparison of mass and electron transfer within overlapped two photocatalysts between the illumination condition with UV light and without UV light.

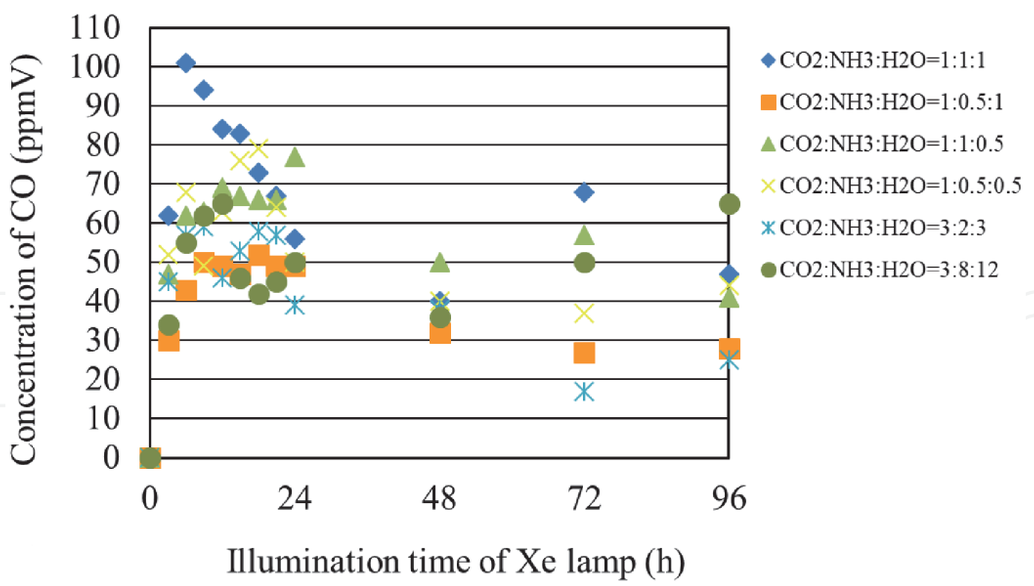

Figure 22.
Comparison of concentration of formed CO among several molar ratios of $CO_2/NH_3/H_2O$ under the illumination condition with UV light.

According to **Figures 22** and **23**, the CO_2 reduction performance is the highest for the molar ratio of $CO_2/NH_3/H_2O$ = 1:1:1.

According to the reaction scheme to reduce CO_2 with H_2O or NH_3 as shown by Eqs. (1)–(5), (13)–(20), the theoretical molar ratio of CO_2/H_2O to produce CO or CH_4 is 1:1 or 1:4, respectively, while that of CO_2/NH_3 to produce CO or CH_4 is 3:2,

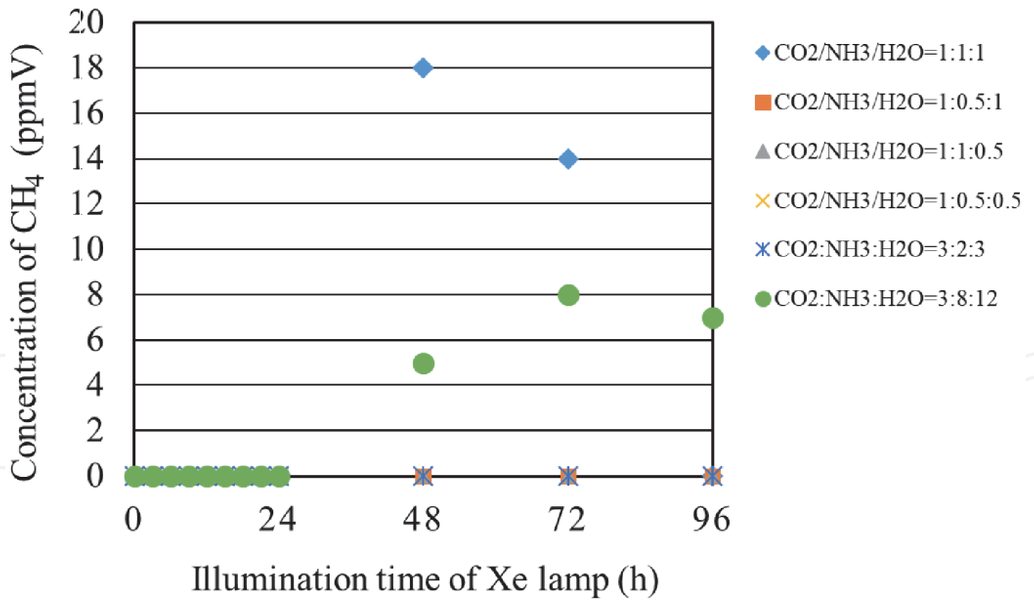

Figure 23.
Comparison of concentration of formed CH_4 among several molar ratios of $CO_2/NH_3/H_2O$ under the illumination condition with UV light.

3:8, respectively. Therefore, this study assumes that the molar ratio of $CO_2/NH_3/H_2O$ = 3:2:3 and 3:8:12 is theoretical molar ratio to produce CO and CH_4, respectively. However, the molar ratio of $CO_2/NH_3/H_2O$ = 1:1:1 is not matched with these theoretical molar ratios to produce CO and CH_4. Since the ionized Cu doped with TiO_2 provides free electron for the reduction reaction process [39], the reductants of NH_3 and H_2O which are less than the values indicated in the theoretical scheme are enough for producing CO and CH_4 in this study. The highest molar quantities of CO and CH_4 per weight of photocatalyst in the reactor, which are obtained for the molar ratio of $CO_2/NH_3/H_2O$ = 1:1:1, are 10.2 and 1.8 μmol/g, respectively.

In addition, it is confirmed from **Figure 22** that the concentration of formed CO is increased from the start of illumination of Xe lamp and decreased after attaining the peak concentration. However, the concentration of formed CO increases again after 48 hours. It is believed that the decrease in the concentration of formed CO is resulted from the oxidization reaction between CO and O_2 which is by-product as shown in Eq. (3) [40]. Since the produced CO might be remained near the photocatalyst due to high absorption performance of netlike glass fiber, this oxidization reaction is thought to be occurred. The increase in the concentration of formed CO after 48 hours might be due to the difference in reaction rates between CO_2/H_2O and CO_2/NH_3 condition. It is also revealed that the maximum concentration of formed CO is higher when the molar of NH_3 is higher than that of H_2O. Since the number of H^+ which can be provided is 3 and 2 for NH_3 and H_2O, respectively, it is considered that NH_3 is effective for promoting the reduction performance of Cu/TiO_2. Furthermore, it is found from **Figures 22** and **23** that the concentration of formed CH_4 starts to increase after the decreasing of CO concentration. According to the reaction schemes, the more H^+ and electron are needed to produce CH_4, resulting that the production of CH_4 starts later.

Figure 24 shows the concentration changes of formed CO along the time under the Xe lamp without UV light. In this experiment, CO is the only fuel produced from the reactions, that is, no CH_4 was detected. Before the experiments, a blank test, which was running the same experiment without illumination of Xe lamp, had been carried out to set up a reference case. No CO or CH_4 was produced in the blank test as expected. According to **Figure 24**, the CO_2 reduction performance is the best

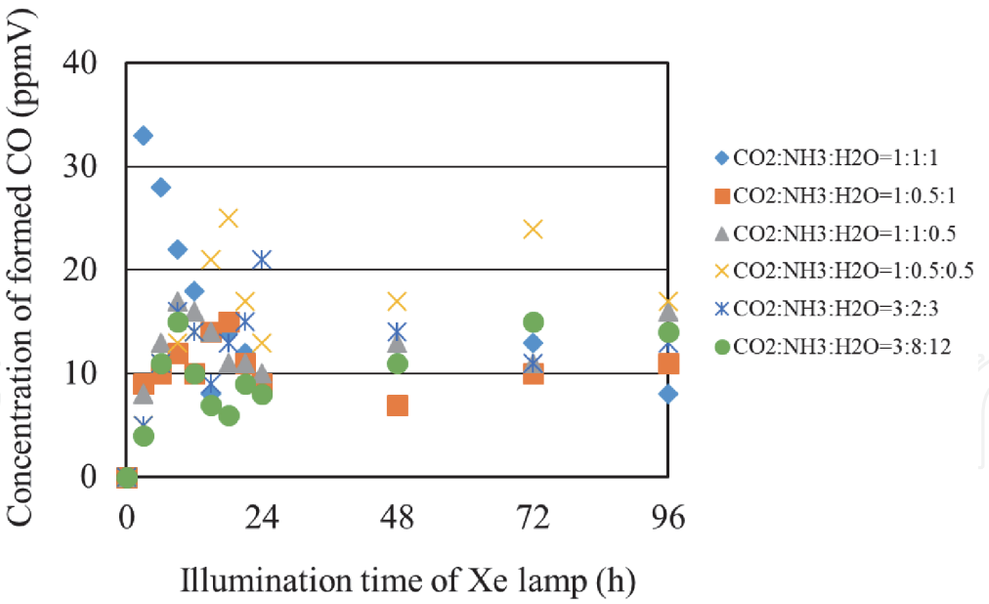

Figure 24.
Comparison of concentration of formed CO among several molar ratios of $CO_2/NH_3/H_2O$ under the illumination condition without UV light.

for the molar ratio of $CO_2/NH_3/H_2O$ = 1:1:1. In addition, it is confirmed from **Figure 24** that the concentration of formed CO is increased from the start of illumination of Xe lamp and decreased after reaching the maximum concentration. However, the concentration of formed CO is increased gradually again after a while. It can be considered that the same reaction mechanism under the illumination condition with UV light as mentioned above occurred.

3.5 Proposal to improve the CO_2 reduction performance with H_2O and H_2 or NH_3

Under the condition of $CO_2/H_2/H_2O$, the highest molar quantity of CO per weight of photocatalyst is 153 μmol/g in a single disc case with UV light illumination. The CO production performance achieved in this study is approximately 500 times as large as that reported in [24, 26] which is owing to Cu doping. The CH_4 production performance achieved in this study is almost the same as that reported in [24]. Since the doped Cu provides the free electron preventing recombination of electron and hole produced as well as the improvement of the light absorption effect, the big improvement of CO_2 reduction performance is obtained in this study.

One way to further promote the CO_2 reduction performance may be that different metals should be doped on the higher and the lower positioned photocatalysts discs. The co-doped such as PbS-Cu/TiO_2, Cu-Fe/TiO_2, Cu-Ce/TiO_2, Cu-Mn/TiO_2, and Cu-CdS/TiO_2 would promote the CO_2 reduction performance of TiO_2 under the CO_2/H_2O condition [7, 9]. When the combination of $CO_2/H_2/H_2O$ is considered, the ion number of dopant is important to match the number of electron emitted from the dopant with H^+ as shown by the reaction schemes of CO_2/H_2O and CO_2/H_2. The same number of electron and H^+ are necessary for fuel production. Though Cu^+ ion is applied to promote the CO_2 reduction performance with TiO_2 in this study, it is expected that the co-doping of Cu and the other metal having larger positive ion might have positive effect for CO_2 reduction with H_2 and H_2O. In addition, the dopant like Fe, which can absorb the shorter wavelength light than Cu [17, 41, 42], should be used at the higher positioned layer. The wavelength of light becomes long

after penetrating the higher positioned photocatalyst [36]. Therefore, it may be an effective way for utilization of wide wavelength range light that the higher positioned Fe/TiO_2 which absorbs the shorter wavelength light and the lower positioned Cu/TiO_2 which absorbs the longer wavelength light are overlapped. This idea is similar to the concept of hybridizing two photocatalysts having different band gaps [13, 42, 43].

On the other hand, under the condition of $CO_2/NH_3/H_2O$, the highest molar quantities of CO and CH_4 per weight of photocatalyst in the reactor, which are obtained for the molar ratio of $CO_2/NH_3/H_2O$ = 1:1:1, are 10.2 and 1.8 μmol/g, respectively. Compared to the previous research on CO_2 reduction with H_2 and H_2O over pure TiO_2, the CO_2 reduction performance of photocatalyst prepared in this study is approximately 35 times as large as that reported in Refs. [24, 39], which is owing to not only Cu doping but also the combination of NH_3 and H_2O. The CO production performance over the Cu/TiO_2 prepared in this study is approximately 3 times as large as that reported in the reference [44]. However, the CH_4 production performance of Cu/TiO_2 prepared in this study is one twentieth as large as that of Cu/TiO_2 reported in the other reference [45]. Therefore, it is necessary to promote the conversion from NH_3 into H_2 in order to improve the reduction performance according to the reaction scheme to reduce CO_2 with NH_3. One way to promote the conversion from NH_3 into H_2 is thought to be using Pt as a dopant. It was reported that Pt/TiO_2 was effective to dissolve NH_3 aqueous solution into N_2 and H_2 [25].

4. Conclusions

The conclusions on this chapter are as follows:

i. Cu in Cu/TiO_2 prepared by this study exists in the form of Cu^+ ion in Cu_2O.

ii. Under the condition of $CO_2/H_2/H_2O$, the highest concentrations of CO and CH_4 produced as well as the highest molar quantities of CO and CH_4 per weight of photocatalyst for Cu/TiO_2 are obtained for $CO_2/H_2/H_2O$ ratio of 1:0.5:0.5. Since the molar ratio of $CO_2/H_2/H_2O$ = 1:0.5:0.5 can be regarded as the molar ratio of CO_2/total reductants = 1:1, it is believed that the results of this study follow the reaction scheme of CO_2/H_2O and CO_2/H_2.

iii. Under the condition of $CO_2/H_2/H_2O$, the highest concentration of CO in two discs case is 1.4 times as large as that in the single disc case, while the highest concentration of CH_4 is 1.7 times with UV light illumination. Under the illumination condition without UV light, the highest concentration of CO with two Cu/TiO_2 disc is 2.8 times as large as that with single Cu/TiO_2 disc.

iv. Under the condition of $CO_2/H_2/H_2O$, the highest molar quantity of CO per weight of photocatalyst with two Cu/TiO_2 discs overlapped is 54% of that with single Cu/TiO_2 disc with UV light illumination. The highest molar quantity of CH_4 per weight of photocatalyst with two Cu/TiO_2 discs overlapped is 65% of that with single Cu/TiO_2 disc.

v. Under the condition of $CO_2/H_2/H_2O$, the molar quantity of CO per weight of photocatalyst with two Cu/TiO_2 discs overlapped is slightly (1.1 times) higher than that with single Cu/TiO_2 disc without UV light illumination.

vi. Under the condition of $CO_2/NH_3/H_2O$, the molar ratio of $CO_2/NH_3/H_2O$ is 1:1:1 under the illumination condition with UV as well as without UV. The highest molar quantities of CO and CH_4 per weight of photocatalyst obtained in this study are 10.2 and 1.8 μmol/g, respectively.

Acknowledgements

The authors would like to gratefully thank from JSPS KAKENHI Grant Number 16K06970 for the financial support of this work.

Author details

Akira Nishimura
Mie University, Tsu, Japan

*Address all correspondence to: nisimura@mach.mie-u.ac.jp

References

[1] Greenhouse Gases Observing Satellite GOAST "IBUSUKI" [Internet]. 2020. Available from: http://www.goast.nies.go.jp/en/ [Accessed: 17 March 2020]

[2] Das S, Daud WMAW. Photocatalytic CO_2 transformation into fuel: A review on advances in photocatalyst and photoreactor. Renewable and Sustainable Energy Reviews. 2014;**39**: 765-805

[3] Adachi K, Ohta K, Mizuno T. Photocatalytic reduction of carbon dioxide to hydrocarbon using copperloaded titanium dioxide. Solar Energy. 1994;**53**:187-190

[4] Tahir M, Amin NS. Photocatalytic reduction of carbon dioxide with water vapor over montmorillonite modified TiO_2 nanocomposites. Applied Catalysis B: Environmental. 2015;**162**:98-109

[5] Tahir M, Amin NS. Indium-doped TiO_2 nanoparticles for photocatalytic CO_2 reduction with H_2O vapors to CH_4. Applied Catalysis B: Environmental. 2015;**162**:98-109

[6] Abdulah H, Khan MMR, Ong HR, Yaakob Z. Modified TiO_2 photocatalyst for CO_2 photocatalytic reduction: An overview. Journal of CO_2 Utilization. 2017;**22**:15-32

[7] Sohn Y, Huang W, Taghipour F. Recent progress and perspectives in the photocatalytic CO_2 reduction of Ti-oxide-based nanomaterials. Applied Surface Science. 2017;**396**:1696-1711

[8] Neatu S, Macia-Agullo JA, Garcia H. Solar light photocatalytic CO_2 reduction: General considerations and selected benchmark photocatalysts. International Journal of Molecular Sciences. 2014;**15**: 5246-5262

[9] Tahir M, Amin NS. Advances in visible light responsive titanium oxide-based photocatalyts for CO_2 conversion to hydrocarbon fuels. Energy Conversion and Management. 2013;**76**:194-214

[10] Ola O, Maroto-Valer MM. Review of material design and reactor engineering on TiO_2 photocatalysis for CO_2 reduction. Journal of Photochemistry and Photobiology. 2015;**24**:16-42

[11] Tan LL, Ong WJ, Chai SP, Mohamed AR. Noble metal modified reduced graphene oxide/TiO_2 ternary nanostructures for efficient visible-light-driven photoreduction of carbon dioxide into methane. Applied Catalysis B: Environmental. 2015;**167**:251-259

[12] Jiao J, Wei Y, Zhao Y, Zhao Z, Duan A, Liu J, et al. AuPd/3DOM-TiO_2 catalysts for photocatalytic reduction of CO_2: High efficient separation of photogenerated charge carriers. Applied Catalysis B: Environmental. 2017;**209**: 228-239

[13] Marci G, Garcia-Lopez EI, Palmisano L. Photocatalytic CO_2 reduction in gas- solid regime in the presence of H_2O by using GaP/TiO_2 composite as photocatalyst under simulated solar light. Catalysis Communications. 2014;**53**:38-41

[14] Beigi AA, Fatemi S, Salehi Z. Synthesis of nanocomposite CdS/TiO_2 and investigation of its photocatalytic activity of CO_2 reduction to CO and CH_4 under visible light irradiation. Journal of CO_2 Utilization. 2014;**7**:23-29

[15] Fang Z, Li S, Gong Y, Liao W, Tian S, Shan C, et al. Comparison of catalytic activity of carbon-based AgBr nanocomposites for conversion of CO_2 under visible light. Journal of Saudi Chemical Society. 2014;**18**:299-307

[16] Nagaveni K, Hegde MS, Madras G. Structure and photocatalytic activity of $Ti_{1-x}M_xO_{2\pm\delta}$ (M = W, V, Ce, Zr, Fe, and

Cu) synthesized by solution combustion method. The Journal of Physical Chemistry B. 2004;**108**:20204-20212

[17] Yoong LS, Chong FK, Dutta BK. Development of copper-doped TiO_2 photocatalyst for hydrogen production under visible light. Energy. 2009;**34**: 1652-1661

[18] Cheng M, Yang S, Chen R, Zhu X, Liao Q, Huang Y. Copper-decorated TiO_2 nanorod thin films in optofluidic planer reactors for efficient photocatalytic reduction of CO_2. International Journal of Hydrogen Energy. 2017;**42**:9722-9732

[19] Khalid NR, Ahmed E, Niaz NA, Nabi G, Ahmad M, Tahir MB, et al. Highly visible light responsive metal loaded N/TiO_2 nanoparticles for photocatalytic conversion of CO_2 into methane. Ceramics International. 2017; **43**:6771-6777

[20] Tan JZY, Fernandez Y, Liu D, Maroto-Valer M, Bian J, Zhang X. Photoreduction of CO_2 using copper-decorated TiO_2 nanorod films with localized surface plasmon behavior. Chemical Physics Letters. 2012;**531**: 149-154

[21] Goren Z, Willner I, Nelson AJ, Frank AJ. Selective photoreduction of CO_2/HCO_3^- to formate by aqueous suspensions and colloids of Pd-TiO_2. The Journal of Physical Chemistry. 1990;**94**:3784-3790

[22] Tseng IH, Chang WC, Wu JCS. Selective photoreduction of CO_2 using sol-gel derived titania and titania-supported copper catalyst. Applied Catalysis B: Environmental. 2002;**37**: 37-38

[23] Nishimura A, Sugiura N, Fujita M, Kato S, Kato S. Influence of preparation conditions of coated TiO_2 film on CO_2 reforming performance. Kagaku Kogaku Ronbunshu. 2007;**33**:146-153

[24] Lo CC, Hung CH, Yuan CS, Wu JF. Photoreduction of carbon dioxide with H_2 and H_2O over TiO_2 and ZrO_2 in a circulated photocatalytic reactor. Solar Energy Materials & Solar Cells. 2007;**33**: 146-153

[25] Nemoto J, Goken N, Ueno H. Photodecomposition of ammonia to dinitrogen and dihydrogen on platinized TiO_2 nanoparticles in an aqueous solution. Journal of Photochemistry and Photobiology A: Chemistry. 2007;**185**: 295-300

[26] Jensen J, Mikkelsen M, Krebs FC. Flexible substrates as basis for photocatalytic reduction of carbon dioxide. Solar Energy Materials & Solar Cells. 2011;**95**:2949-2958

[27] Nishimura A, Toyoda R, Tatematsu D, Hirota M, Koshio A, Kokai F, et al. Optimum reductants ratio for CO_2 reduction by overlapped Cu/ TiO_2. Materials Science. 2019;**6**:214-233

[28] Nishimura A, Sakakibara Y, Inoue T, Hirota M, Koshio A, Kokai F, et al. Impact of molar ratio of NH_3 and H_2O on CO_2 reduction performance over Cu/TiO_2 photocatalyst. Physics & Astronomy International Journal (PAIJ). 2019;**3**:176-182

[29] Nishimura A, Tatematsu D, Toyoda R, Hirota M, Koshio A, Kokai F, et al. Effect of overlapping layout of Fe/ TiO_2 on CO_2 reduction with H_2 and H_2O. MOJ Solar and Photoenergy Systems (MOJSP). 2019;**3**:1-8

[30] Japan society of mechanical engineering. Heat Transfer Hand Book. 1st ed. Maruzen; 1993. pp. 367-369

[31] Yang G, Cheng S, Li C, Zhong J, Ma C, Wang Z, et al. Investigation of the oxidation states of Cu additive in colored borosilicate glasses by electron energy loss spectroscopy. Journal of Applied Physiology. 2014;**116**. DOI: 10.1063/1.4903955

[32] Qin S, Xin F, Liu Y, Yin X, Ma W. Photocatalytic reduction of CO_2 in methanol to methyl formate over CuO-TiO_2 composite catalysts. Journal of Colloid and Interface Science. 2011;**356**: 257-261

[33] Liu L, Gao F, Zhao H, Li Y. Tailoring Cu valence and oxygen vacancy in Cu/TiO_2 catalysts for enhanced CO_2 photoreduction efficiency. Applied Catalysis B: Environmental. 2013; **134-135**:349-358

[34] EELS data base [Internet]. 2020. Available from: https//eesdb.eu/spectra/titanium-dioxide-2/ [Accessed: 18 March 2020]

[35] Hinojosa-Reyes M, Camposeco-Solis R, Zanella R, Zanella R, Gonzalez VR. Hydrogen production by tailoring the brookite and Cu_2O ratio of sol-gel Cu-TiO_2 photocatalysts. Chemosphere. 2017;**184**:992-1002

[36] Nishimura A, Zhao X, Hayakawa T, Ishida N, Hirota M, Hu E. Impact of overlapping Fe/TiO_2 prepared by sol-gel and dip-coating process on CO_2 reduction. International Journal of Photoenergy. 2016;**2016**. DOI: 10.1155/2016/2392581

[37] Nishimura A, Komatsu N, Mitsui G, Hirota M, Hu E. CO_2 reforming into fuel using TiO_2 photocatalyst and gas separation membrane. Catalysis Today. 2009;**148**:341-349

[38] Nishimura A, Okano Y, Hirota M, Hu E. Effect of preparation condition of TiO_2 film and experimental condition on CO_2 reduction performance of TiO_2 photocatalyst membrane reactor. International Journal of Photoenergy. 2011;**2011**. DOI: 10.1155/2011/305650

[39] Paulino PN, Salim VMM, Resende NS. Zn-Cu promoted TiO_2 photocatalyst for CO_2 reduction with H_2O under UV light. Applied Catalysis B: Environmental. 2016;**185**:362-370

[40] Tahir M, Amin NAS. Photo-induced CO_2 reduction by hydrogen for selective CO evolution in dynamic monolith photoreactor loaded with Ag-modified TiO_2 nanocatalyst. International Journal of Hydrogen Energy. 2017;**42**: 15507-15522

[41] Ambrus Z, Balazs N, Alapi T, Wittmann G, Sipos P, Dombi A, et al. Synthesis, structure and photocatalytic properties of Fe(III)-doped TiO_2 prepared from $TiCl_3$. Applied Catalysis B: Environmental. 2008;**81**:27-37

[42] Navio JA, Colon G, Litter MI, Bianco GN. Synthesis, characterization and photocatalytic properties of iron-doped titania semiconductors prepared from TiO_2 and iron (III) acetylacetonate. Journal of Molecular Catalysis A: Chemical. 1996;**106**:267-276

[43] Song G, Xin F, Chen J, Yin X. Photocatalytic reduction of CO_2 in cycohexanol on CdeS-TiO_2 heterostructured photocatalsyt. Applied Catalysis A: General. 2014;**473**:90-95

[44] Aguirre ME, Zhou R, Engene AJ, Guzman MI, Grela MA. Cu_2O/TiO_2 heterostructures for CO_2 reduction through a direct Z-scheme: Protecting Cu_2O from photocorrosion. Applied Catalysis B: Environmental. 2017;**217**: 485-493

[45] Ambrozova N, Reli M, Sihor M, Kustrowski P, Wu JCS, Koci K. Copper and platinum doped titania for photocatalytic reduction of carbon dioxide. Applied Surface Science. 2018; **430**:475-487